

Proceedings of the ASME 2021 16th International Manufacturing Science and Engineering Conference MSEC2021

June 21-25, 2021, Virtual, Online

MSEC2021-63916

CREATION OF FUNCTIONALLY GRADED GLASS CHANNELS BY ELECTROCHEMICAL DISCHARGE MACHINING PROCESS: A FEASIBILITY STUDY

Andrea Grisell, Murali Sundaram¹

Department of Mechanical and Materials Engineering, University of Cincinnati Cincinnati, OH

ABSTRACT

Functionally graded surfaces – surfaces with properties that are engineered to have spatial variations – have numerous applications such as micropumps, auto-mixers, and flow control for lab-on-chip devices. Manufacturing of functionally graded surfaces is an increasingly important topic of research. This study investigates the feasibility of creating a functionally graded surface during channeling of borosilicate glass by the electrochemical discharge machining (ECDM) process. The ability to create surface roughness gradients in microchannels during the machining process was demonstrated by modifying the input voltage, tool feed rate, and tool rotation speed. Microchannels with graded surface roughness having Ra values ranging from 0.35 to 4.07 µm were successfully machined on borosilicate glass by ECDM. Surface profiles were obtained via a stylus profilometer, and roughness values were calculated after detrending and applying a Gaussian filter. To demonstrate the process versatility, micro channels with increasing and decreasing Ra values were machined, one increasing from 1.43 μ m to 4.07 μ m, another decreasing from 3.29 μ m to 1.10 μ m. To demonstrate the process repeatability, a micro channel with similar surface roughness on both ends and a lower Ra value in the center was created. In this channel, the Ra value at the start is $0.35 \mu m$, reducing to $0.24 \mu m$, then rising again to $0.38 \mu m$ in the final section.

Keywords: Electrochemical discharge machining, ECDM, microchannels, functionally graded surface

1. INTRODUCTION

Functionally graded materials (FGM) are materials whose composition or properties are designed to vary from one area to another. Examples of FGM can be found in thermal barrier coatings on turbine blades [1], some density-graded solar cells [2], bio-active coatings for medical purposes [3,4], and many others. However, there are cases where it is desirable to grade

only the surface properties of a feature, such as for mixing in microchannels [5]. Lab-on-chip technologies increasingly have a need for simple ways to control fluid flow through increasingly smaller channels.

The effect of surface geometry on fluid flow, particularly in microchannels, has been well documented in literature [6-12]. It was reported that the effect of surface roughness on the pressure drop increases significantly at the micro scale [7]. One study reported the use of a surface roughness gradient as part of a micropump design [10] and another demonstrated the effective use of structured rough surfaces to guide droplet movement [11]. These studies primarily utilized deterministic features such as regularly spaced pillars to create a defined surface roughness. However, one study investigated the effects of random surface roughness resulting from mircomilling on blood flow through microchannels, and found that there was a significant drop in the apparent viscosity of blood and water in the milled surfaces [12]. As concluded in these works and others, surface geometry plays a large role in the behavior of fluids in microchannels.

The microchannels in this study are created in borosilicate glass. Glass is a highly desirable material, especially in the biomedical field, for its optical properties, chemical inertness, and heat resistance [13-15]. However, it is relatively difficult to machine, particularly at the microscale [15,16]. Electrochemical discharge machining (ECDM) provides a nontraditional way to machine nonconducting materials such as glass at the micro scale. ECDM is a process in which a DC voltage is applied across two electrodes submerged in an electrolyte. The machining tool acts as the cathode, and the anode is a larger electrode. Due to electrolysis, gas bubbles begin to form around the tool, eventually coalescing to create a gas film. Once a critical voltage is reached, sparks occur at the tool, leading to material removal of the nearby workpiece via melting, vaporization, and chemical action due to the localized rapid heating of electrolyte [17-19]. A schematic of this process is shown in Figure 1.

¹ Contact author: murali.sundaram@uc.edu

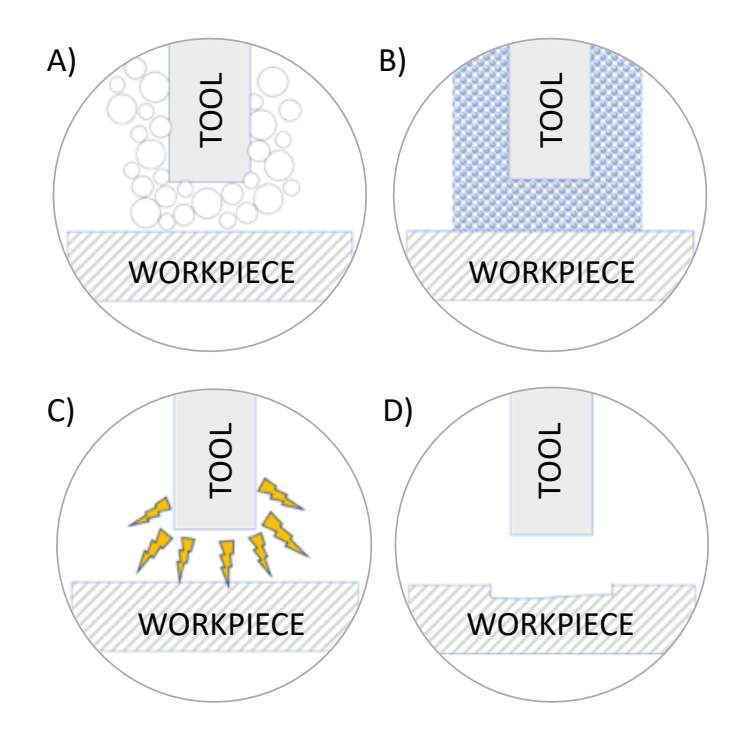


FIGURE 1: Schematic of ECDM mechanism. (A) Electrolysis forms gas bubbles around the tool. (B) Bubbles coalesce to form an isolating gas film. (C) Spark discharge occurs. (D) Workpiece material is removed.

Some studies have looked at the surface morphologies resulting from different process parameters such as tool feed rate, electrolyte concentration, applied voltage, etc. [20,21]. The objective of this study is to demonstrate that the surface roughness resulting from machining microchannels via ECDM can be explicitly controlled to create functionally graded channels during the machining process. It is known that channel wall roughness is linked with hydrophobicity and greatly affects flow rate at the microscale [8,22], thus the flow properties can be controlled to an extent without the use of external forces. This has potential applications for a number of microfluidic purposes such as lab-on-chip devices and auto-mixers.

2. MATERIALS AND METHODS

The 3-axis micro-ECDM setup is detailed in Figures 2 and 3. The tool—a 0.5 mm tungsten carbide rod—was mounted in a spindle attached to a micro-stepper motor acting as the Z-axis. The borosilicate glass workpiece was fixtured in an acrylic tank whose X-Y position was controlled by two more micro-stepper motors. To provide a pulsed voltage, the DC power supply was connected to a pulse width modulator (PWM). The frequency and duty cycle were set to 300 Hz and 50%, respectively [23]. The anode was a Ti-6Al-4V plate, and the tool-workpiece gap was set to a nominal 45 μ m. The tank was then filled with 0.5 molar sodium hydroxide such that the length of tool immersed in the electrolyte was 2 mm [23,24].

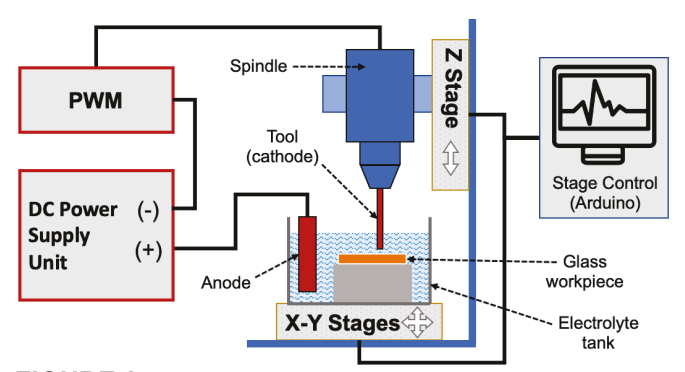


FIGURE 2: Schematic of micro ECDM setup.

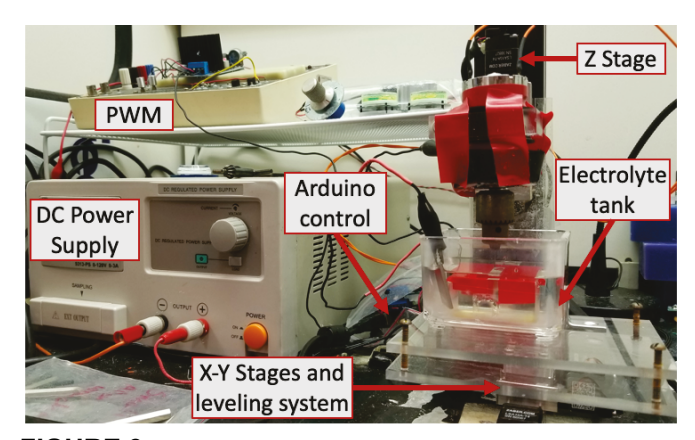


FIGURE 3: Experimental ECDM setup.

Experiments consisted of varying voltage, feed rate, and tool rotation speed at set intervals to create distinct sections within a machined channel, denoted as "Section A", "Section B", etc. Each parameter set was used to machine for a distance of 3 mm so the analysis of the final surface would not be affected by end conditions of the channel or transition zones between sections. For example, a channel that is graded using two tool rotation speeds (measured in rotations per minute, or RPM) began machining with the first RPM setting and after 3 mm of machining had been completed, the system was switched to the second RPM setting without stopping or interrupting the machining process.

2.1 Data Analysis

The surfaces in this study are characterized by obtaining a profile with a profilometer, then surface roughness was quantified by the arithmetical mean deviation (Ra). The surface profile of each machined channel was obtained using a Mitutoyo SJ-410 stylus profilometer. Using MATLAB, the profile was first detrended to compensate for tilt in the system before applying a Gaussian filter [25]. In order to eliminate waviness caused by the eccentricity of the stage, the cut-off value was set to 0.3048 mm—the known eccentricity of the stage's lead screw. The resulting profile was taken as the mean line, and the roughness profile was calculated as the resultant high-pass component. Some samples were also imaged using a scanning electron microscope (SEM) after sputtering with gold.

3. RESULTS AND DISCUSSION

Two-section channels were machined, demonstrating the ability to significantly change the surface roughness during machining. Figure 4 shows a channel in which the surface roughness significantly decreases from the first section to the second. This channel was machined with constant applied voltage of 75 V and tool rotation of 1200 RPM while the tool feed rate was varied. The first section was machined at a feed rate of $2.0~\mu\text{m/s}$, which was increased to $6.0~\mu\text{m/s}$ after a set time to create the second section. The calculated Ra values are $1.93~\mu$ and $1.05~\mu$ m, respectively. The green highlighted portions of the profile show the data used to calculate the roughness parameters. The SEM images highlight the differences in the surfaces of the two sections, with Section A showing more asperities, possibly caused by the increased number of sparks per area due to the slower feed rate [26].

Figure 5 shows another channel where the Ra value drastically increases between sections. The applied voltage and tool feed rate were held constant at 75 V and 6.0 μ m/s, respectively. Machining began with a tool rotation speed of 1200 RPM, which was then turned off for Section B. The resulting Ra

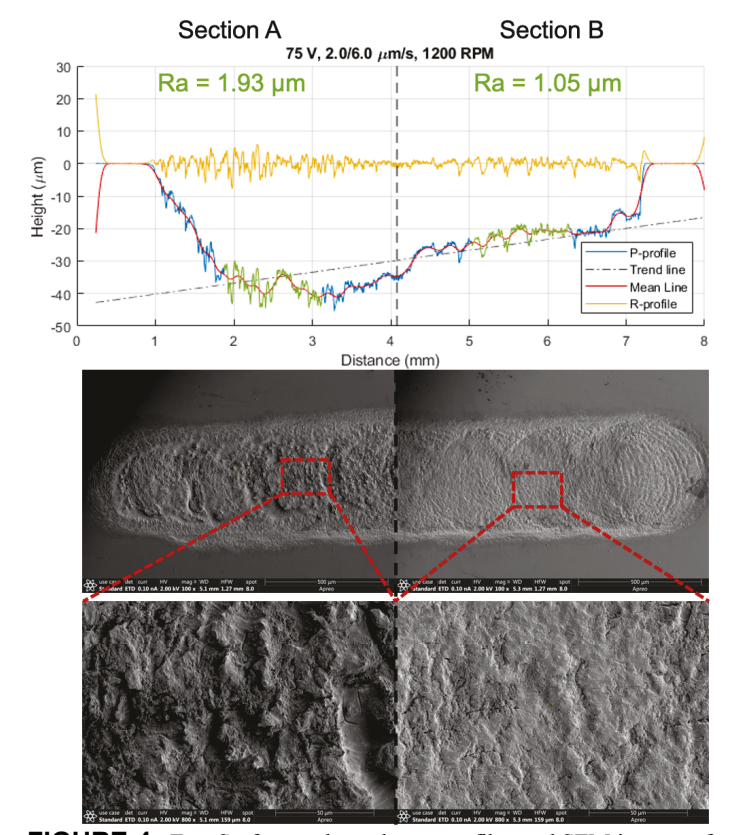


FIGURE 4: *Top:* Surface and roughness profiles and SEM images of two-section functionally graded channel with decreasing surface roughness. Machining parameters were input voltage of 75 V and tool rotation speed of 1200 RPM. The feed rate began at 2.0 μ m/s, then changed to 6.0 μ m/s after 3 mm were machined. *Bottom:* SEM images of surfaces.

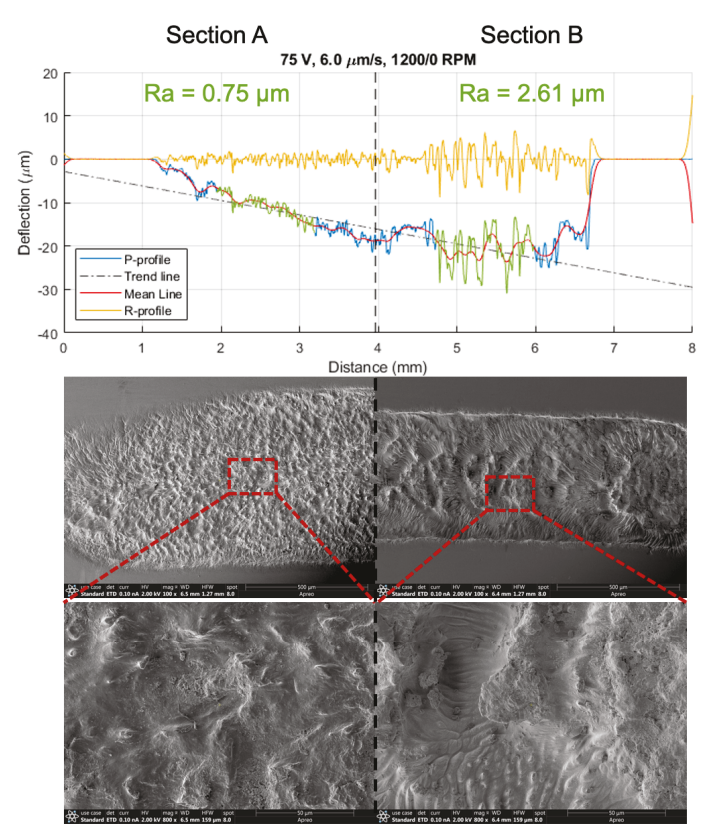


FIGURE 5: *Top:* Surface and roughness profiles and SEM images of two-section functionally graded channel with increasing surface roughness. Machining parameters were input voltage of 75 V, tool feed rate of 6.0 μ m/s, and tool rotation speed of 1200 RPM. After 3mm, the tool rotation was turned off to create the second section. *Bottom:* SEM images of surfaces.

values were 0.75 and 2.61 μm , respectively. The SEM images show glass re-melt in Section B not seen in Section A, likely the result of the lack of tool rotation.

Tool rotation is known to improve the circulation of the electrolyte and to help clear out debris from material removal, and it avoids discharge energy being focused in one area [27]. This explains the high instance of glass remelt areas found in Section B, but not Section A. It has been reported that increasing the tool rotational speed effectively decreased surface roughness, as the gas film thickness becomes thinner and more homogenous with increasing tool rotation [28].

Expanding on the results of the two-section channels, Figure 6 shows a three-section channel with a more gradual decrease in surface roughness. This gradient was created by increasing tool rotation as machining progressed from 0 to 1200 to 3000 RPM while applied voltage and feed rate were held constant at 80 V and 10.0 $\mu m/s$, respectively, again demonstrating the effects of tool rotation on surface roughness.

In contrast, by instead increasing the machining voltage in increments of 5 V (70, 75, then 80 V) while feed rate was held at 10.0 μ m/s and rotation was set to 3000 RPM, another channel was made with gradually increasing roughness (Figure 7). The higher voltage results in an increase in the rate of gas bubble

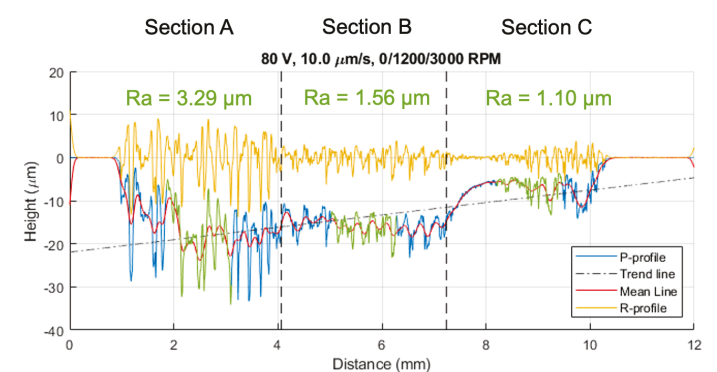


FIGURE 6: Surface and roughness profiles of 3-section channel machined at 80 V, feed rate of 10 μ m/s, with tool rotation speeds varying from 0 RPM in Section A to 1200 RPM in Section B to 3000 RPM in Section C.

formation, leading to more spark generation [29]. This means that at higher applied voltage, there is higher discharge energy, leading to a higher material removal rate (MRR). At the same feed rate as in Sections A and B, the higher MRR caused increased surface roughness.

To demonstrate the process repeatability, a micro channel was successfully machined with an "A-B-A" pattern—the surface roughness on the ends of channel is roughly equal, while the center section has a lower Ra value. This channel was made by varying the feed rate, beginning at 4.0 $\mu m/s$, increasing to 6.0 $\mu m/s$ for Section B, then ending with 10.0 $\mu m/s$ in the final section, shown in Figure 8. The applied voltage was a constant 75 V and tool rotation was set at 3000 RPM.

The reason different feed rates were required to achieve similar roughness values for Sections A and C is likely due to the extended machining time. The setup used is a closed system, resulting in the temperature of the electrolyte increasing over time, which is known to increase the conductivity of the electrolyte and to affect the gas film [21,30,31]. It should be noted that both increasing and decreasing surface roughness gradients were achieved, implying that while temperature of the electrolyte is an important factor, it does not dominate these results.

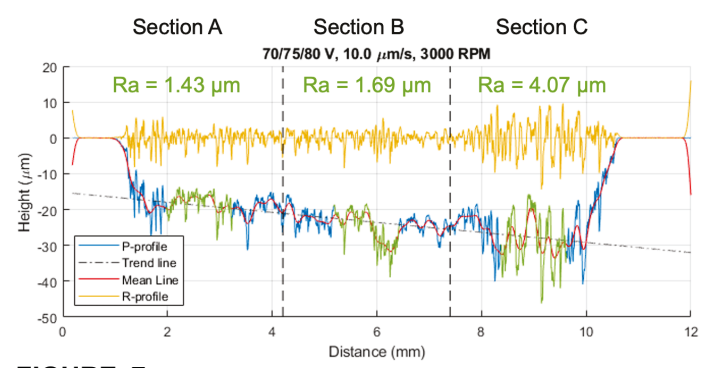


FIGURE 7: Surface and roughness profiles of 3-section channel machined at a feed rate of 10 μ m/s, tool rotation speed of 3000 RPM and three voltage settings: 70 V, 75 V, then 80 V in Sections A, B, and C, respectively.

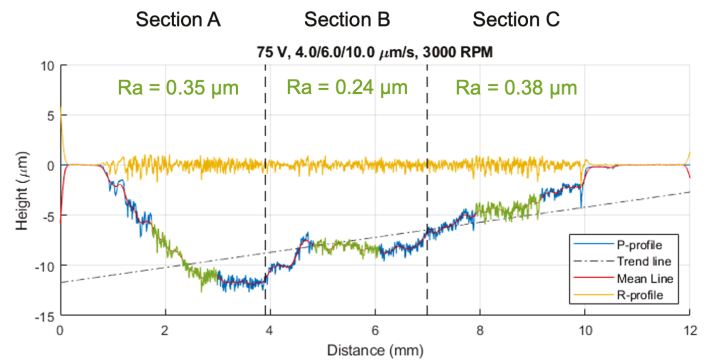


FIGURE 8: Surface profiles of "A-B-A" three-section channel with lower surface roughness in the center, and equal roughness on both ends. The channel was machined at 75 V, 3000 RPM tool rotation, and with 4.0, 6.0, and 10.0 μm/s feed rates for Sections A, B, and C respectively.

4. CONCLUSION

This study has successfully demonstrated the ability to create a functionally graded channel in glass with a single ECDM operation. By adjusting standard machining variables such as voltage, feed rate, and tool rotation speed, we were able to control the resultant surface roughness. This provides a simple way to not only tailor the surface geometry of glass microchannels without necessitating a second process, it also demonstrates that a specified surface roughness gradient can be produced simultaneously to machining.

ACKNOWLEDGEMENTS

Financial support provided by the National Science Foundation under Grant No. CMMI-1833112 is acknowledged.

REFERENCES

- [1] Mahamood, Rasheedat M., et al. "Functionally graded material: an overview." Proceedings of the World Congress on Engineering 2012 Vol III WCE 2012, July 4 6, 2012, London, U.K..
- [2] Yuan, Hao-Chih, et al. "Efficient black silicon solar cell with a density-graded nanoporous surface: Optical properties, performance limitations, and design rules." Applied Physics Letters 95.12 (2009): 123501.
- [3] Gomez-Vega, Jose M., et al. "Novel bioactive functionally graded coatings on Ti6Al4V." Advanced Materials 12.12 (2000): 894-898.
- [4] Kim, H-M., et al. "Graded surface structure of bioactive titanium prepared by chemical treatment." Journal of Biomedical Materials Research 45.2 (1999): 100-107.
- [5] Farshchian, Bahador, et al. "3D Nanomolding and Fluid Mixing in Micromixers with Micro-Patterned Microchannel Walls." Nano Convergence, vol. 4, no. 1, 2017, pp. 1-10.
- [6] Weaver, S. A., Michael David Barringer, and Karen Ann Thole. "Microchannels with manufacturing roughness levels." Journal of turbomachinery 133.4 (2011).

- [7] Ranjan, Prabhat. "Investigations on the flow behaviour in microfluidic device due to surface roughness: a computational fluid dynamics simulation." Microsystem Technologies 25.10 (2019): 3779-3789.
- [8] Sbragaglia, M., et al. "Surface roughness-hydrophobicity coupling in microchannel and nanochannel flows." Physical review letters 97.20 (2006): 204503.
- [9] Chen, Yongping, et al. "Role of surface roughness characterized by fractal geometry on laminar flow in microchannels." Physical Review E 80.2 (2009): 026301.
- [10] Cheng, Chih-Ming, and Cheng-Hsien Liu. "An electrolysis-bubble-actuated micropump based on the roughness gradient design of hydrophobic surface." Journal of microelectromechanical systems 16.5 (2007): 1095-1105.
- [11] Shastry, Ashutosh, Marianne J. Case, and K. F. Bohringer. "Engineering surface roughness to manipulate droplets in microfluidic systems." 18th IEEE International Conference on Micro Electro Mechanical Systems, 2005. MEMS 2005. IEEE, 2005.
- [12] Prentner, S., et al. "Effects of channel surface finish on blood flow in microfluidic devices." Microsystem technologies 16.7 (2010): 1091-1096.
- [13] Ren, Kangning, Jianhua Zhou, and Hongkai Wu. "Materials for microfluidic chip fabrication." Accounts of chemical research 46.11 (2013): 2396-2406.
- [14] Ren, Juan, Baskar Ganapathysubramanian, and Sriram Sundararajan. "Experimental analysis of the surface roughness evolution of etched glass for micro/nanofluidic devices." Journal of Micromechanics and Microengineering 21.2 (2011): 025012.
- [15] Martins, João Pedro, Giulia Torrieri, and Hélder A. Santos. "The importance of microfluidics for the preparation of nanoparticles as advanced drug delivery systems." Expert opinion on drug delivery 15.5 (2018): 469-479.
- [16] Rodriguez, Indalesio, et al. "Rapid prototyping of glass microchannels." Analytica Chimica Acta 496.1-2 (2003): 205-215.
- [17] Basak, Indrajit, and Amitabha Ghosh. "Mechanism of material removal in electrochemical discharge machining: a theoretical model and experimental verification." Journal of materials processing technology 71.3 (1997): 350-359.
- [18] Kolhekar, Ketaki Rajendra, and Murali Sundaram. "Study of gas film characterization and its effect in electrochemical discharge machining." Precision Engineering 53 (2018): 203-211.
- [19] Wüthrich, Rolf, and Valia Fascio. "Machining of non-conducting materials using electrochemical discharge phenomenon—an overview." International Journal of Machine Tools and Manufacture 45.9 (2005): 1095-1108.

- [20] Ziki, J.D. Abou, T. F. D, and Rolf Wüthrich. "Microtexturing channel surfaces on glass with spark assisted chemical engraving." International Journal of Machine Tools and Manufacture 57 (2012): 66-72.
- [21] Kolhekar, Ketaki Rajendra, and Murali Sundaram. "A study on the effect of electrolyte concentration on surface integrity in micro electrochemical discharge machining." Procedia CIRP 45. Supplement C (2016): 355-358.
- [22] Kleinstreuer, C., and J. Koo. "Computational analysis of wall roughness effects for liquid flow in microconduits." Journal of Fluids Engineering 126.1 (2004): 1-9.
- [23] Sundaram, Murali, Yu-Jen Chen, and K. Rajurkar.
 "Pulse electrochemical discharge machining of glass-fiber epoxy reinforced composite." CIRP Annals (2019).
- [24] Cheng, Chih-Ping, et al. "Study of gas film quality in electrochemical discharge machining." International Journal of Machine Tools and Manufacture 50.8 (2010): 689-697.
- [25] Luo, N. L., P. J. Sullivan, and Kenneth J. Stout. "Gaussian filtering of three-dimensional engineering surface topography." Measurement Technology and Intelligent Instruments. Vol. 2101. International Society for Optics and Photonics, 1993.
- [26] Nguyen, Khac-Ha, Pyeong An Lee, and Bo Hyun Kim. "Experimental investigation of ECDM for fabricating micro structures of quartz." International journal of precision engineering and manufacturing 16.1 (2015): 5-12.
- [27] Zheng, Zhi-Ping, et al. "The tool geometrical shape and pulse-off time of pulse voltage effects in a Pyrex glass electrochemical discharge microdrilling process." Journal of Micromechanics and Microengineering 17.2 (2007): 265.
- [28] Zheng, Zhi-Ping, et al. "3D microstructuring of Pyrex glass using the electrochemical discharge machining process." Journal of micromechanics and microengineering 17.5 (2007): 960.
- [29] Bhattacharyya, B., B. N. Doloi, and S. K. Sorkhel. "Experimental investigations into electrochemical discharge machining (ECDM) of non-conductive ceramic materials." Journal of Materials Processing Technology 95.1-3 (1999): 145-154.
- [30] Ho, Patience C., Donald A. Palmer, and Robert H. Wood. "Conductivity measurements of dilute aqueous LiOH, NaOH, and KOH solutions to high temperatures and pressures using a flow-through cell." The Journal of Physical Chemistry B 104.50 (2000): 12084-12089.
- [31] Han, Min-Seop, Byung-Kwon Min, and Sang Jo Lee. "Modeling gas film formation in electrochemical discharge machining processes using a side-insulated electrode." Journal of Micromechanics and Microengineering 18.4 (2008): 045019.